CHALMERS | UNIVERSITY OF GOTHENBURG

PREPRINT 2008:14

Fatigue damage assessment for a spectral model of non-Gaussian random loads

SOFIA ÅBERG
KRZYSZTOF PODGÓRSKI
IGOR RYCHLIK

Department of Mathematical Sciences
Division of Mathematical Statistics
CHALMERS UNIVERSITY OF TECHNOLOGY
UNIVERSITY OF GOTHENBURG
Göteborg Sweden 2008

Preprint 2008:14

Fatigue damage assessment for a spectral model of non-Gaussian loads

Sofia Åberg, Krzysztof Podgórski, Igor Rychlik

Department of Mathematical Sciences
Division of Mathematical Statistics
Chalmers University of Technology and University of Gothenburg
SE-412 96 Göteborg, Sweden
Göteborg, March 2008

Preprint 2008:14
ISSN 1652-9715

Matematiska vetenskaper
Göteborg 2008

Fatigue damage assessment for a spectral model of non-Gaussian random loads

Sofia Åberg [a,*], Krzysztof Podgórski [b], Igor Rychlik [a]

[a] *Mathematical Sciences, Chalmers University of Technology, SE-412 96, Gothenburg, Sweden*

[b] *Centre for Mathematical Sciences, Mathematical Statistics, Lund University, Box 118, SE-221 00 Lund, Sweden*

Abstract

In this paper a new model for random loads – the Laplace driven moving average – is presented. The model is second order, non-Gaussian, and strictly stationary. It shares with its Gaussian counterpart the ability to model any spectrum but has additional flexibility to model the skewness and kurtosis of the marginal distribution. Unlike most other non-Gaussian models proposed in the literature, such as the transformed Gaussian or Volterra series models, the new model is no longer derivable from Gaussian processes. In the paper a summary of the properties of the new model is given and its upcrossing intensities are evaluated. Then it is used to estimate fatigue damage both from simulations and in terms of an upper bound that is of particular use for narrowband spectra.

Key words: fatigue damage, Laplace distribution, spectral density, Rice's formula, moving average, non-Gaussian process

1 Introduction

For a long time the study of random loads has been dominated by Gaussian processes. However, many real loads, e.g. ocean waves, show considerable non-Gaussian features such as a skewed marginal distribution with heavy tails. For mooring lines, for instance, loads often exhibit significant asymmetry having skewness about 0.8, see [1]. A serious consequence of not taking this into

* Corresponding author. *Phone:* +46 31 772 35 82. *Fax:* +46 31 772 35 08.
Email addresses: abergs@chalmers.se (Sofia Åberg), krys@maths.lth.se (Krzysztof Podgórski), rychlik@chalmers.se (Igor Rychlik).

account in a fatigue application is that the fatigue life predictions from the model may be far too long, as reported by [2], [3], [4], [5] and [6]. In order to overcome this problem a lot of effort has been made to find suitable non-Gaussian models.

One solution to this problem that has been proposed by [7] is the class of transformed Gaussian processes. These processes take their starting point in a Gaussian process $Z(t)$ and a continuous and increasing function g, say. Then one forms a non-Gaussian process according to $Y(t) = g(Z(t))$. In this way the process $Y(t)$ can have a non-Gaussian marginal distribution. Different strategies to choose the function g have been proposed and studied in [8], [9], [10] and [11]. An advantage with the transformed Gaussian models is that they are easy to simulate from and that the fatigue damage can be related to Gaussian loads where a lot of results are known. A serious disadvantage, however, is that the spectral density function is modified when the transformation is applied. As reported in [12] this can be particularly unfortunate when the process is used as an input to a linear filter since in such a case the presence of resonances can lead to large errors in the predicted fatigue damage.

Another, and more complex, approach to non-Gaussian processes are obtained by Volterra series expansions which can be described as higher order transformations of Gaussian loads. Considerable effort has been made to study these kind of processes and examples thereof can be found in [13] and the recent study [14].

It is common for the just described models that they take Gaussian processes as their starting point. In this paper we take another approach and study a model for random loads which fundamentally goes beyond the Gaussian theory. Still, as in the Gaussian case, the main tool for the new model is the spectral theory. However in addition to the spectrum, the model also has two more parameters for skewness and kurtosis of the marginal distribution. In this way it offers an alternative to the transformed Gaussian models that is preserving the correct spetrum. Both simulating from the model and passing through linear filters are straightforward. The purpose of the paper is to present the most fundamental properties and also show through examples how the model can be used to estimate fatigue damage.

2 Rainflow damage

The rainflow method was first introduced by Endo [15] in the 1960's. His approach has then been modified by others to make it more suitable for statistical analysis and here the definition of the rainflow cycle given in [16] will be used.

Assume that $Y(t)$, $t \in [0,T]$ is a variable load having a finite number of local maxima and assume that each local maximum $v_i = Y(t_i)$ in $Y(t)$ is paired with a particular local minimum u_i, determined as follows:

(1) From the ith local maximum (having value v_i) one determines the lowest values in forward and backward directions between t_i and the nearest points at which $Y(t)$ exceeds v_i.
(2) The larger of those two values, denoted by u_i^{rfc}, is the rainflow minimum paired with v_i, i.e. u_i^{rfc} is the smallest drop before reaching the value v_i again on either side, see Figure 1 for an illustration. The cycle range is defined as $S_i = v_i - u_i^{\text{rfc}}$.

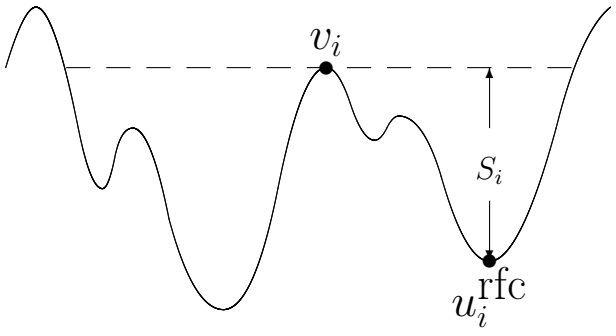

Fig. 1. A rainflow pair.

Note that for some local maxima v_i, the corresponding rainflow minimum u_i^{rfc} could be located outside the interval $[0,T]$. In such situations, the incomplete rainflow cycle constitutes the so called residual and has to be handled separately. In this approach we assume that, in the residual, the maxima form cycles with the preceding minima.

The total damage $D(T)$, defined using the rainflow method and applying the linear Palmgren-Miner ([17], [18]) damage accumulation rule, leads to

$$D(T) = \sum f(u_i^{\text{rfc}}, v_i) + D^{\text{res}}, \tag{1}$$

where $f(u_i^{\text{rfc}}, v_i)$ is the fatigue damage due to the rainflow pair (u_i^{rfc}, v_i) and D^{res} is the damage caused by cycles found in the residual. In this study, we assume that $f(u_i^{\text{rfc}}, v_i)$ is typically of the form $f(u_i^{\text{rfc}}, v_i) = \alpha(v_i - u_i^{\text{rfc}})^\beta$, where $\alpha > 0$ and $\beta \geq 1$ are experimentally defined fatigue parameters.

If the load is a random process, then one is rather interested in computing the expected damage. As discussed in the appendix, it is convenient to express the damage in terms of the intensity of upcrossings of intervals. Unfortunately, it is in most cases very hard to compute this intensity and explicit formulas are known only for loads satisfying a Markov condition. However, the intensity

can be bounded by the intensity of upcrossings of a level which is given by the celebrated Rice's formula [19]

$$\mu^+(u) = \int_0^{+\infty} z f_{Y(0),\dot{Y}(0)}(u, z)\, dz, \tag{2}$$

where $f_{Y(0),\dot{Y}(0)}(u, z)$ is the joint probability density function of the process at time zero $Y(0)$ and its derivative $\dot{Y}(0)$. Thus, summarizing the discussion in the appendix, if $\mu^+(u)$ is known then the fatigue damage can be conveniently bounded from above.

3 The Laplace driven moving average model

The proposed new class of models for loads is, unlike most other models, not related to Gaussian processes. However, it still has finite variance and consequently a spectrum corresponding to its correlation structure. It can also be viewed as a generalization of Gaussian processes as the latter can be obtained by proper specification of parameters. Moreover, the model contains two more parameters defining the third or fourth moments or, equivalenty, the skewness and kurtosis. This allows for modeling using spectral densities and at the same time having a skewed marginal distribution with tails that are heavier than the Gaussian ones.

3.1 Definition and properties

The model we propose for loads is a continuous time moving average (MA) which may be written as

$$Y(t) = \int_{-\infty}^{\infty} f(t - x)\, d\Lambda(x), \tag{3}$$

where $f(x)$ will be referred to as a kernel function and $\Lambda(x)$ is a stochastic process having independent and stationary increments having a generalized asymmetric Laplace distribution soon to be defined. The process $\Lambda(x)$ is referred to as *Laplace motion* and the resulting process $Y(t)$ is called the *Laplace driven moving average*. Thus $Y(t)$ may be thought of as a convolution of f with the increments of the process $\Lambda(x)$. A process generated in this way is stationary and ergodic. If $\Lambda(x)$ is chosen to be a Brownian motion, then $Y(t)$ becomes a Gaussian process, while in general it is non-Gaussian.

The generalized asymmetric Laplace distribution, sometimes called Bessel function distribution, is easiest defined by its characteristic function. More precisely, a random variable Z is said to have a generalized asymmetric Laplace

distribution if its characteristic function is given by

$$\phi_Z(v) = \mathsf{E}[e^{ivZ}] = \frac{e^{iv\theta}}{(1 - i\mu v + \frac{\sigma^2 v^2}{2})^{\frac{1}{\nu}}},$$

where θ, $\mu \in \mathbb{R}$ and ν, $\sigma > 0$ are parameters. If $\mu = 0$ the distribution is symmetric and otherwise it is asymmetric. An extensive overview of Laplace distributions can be found in [20]. The generalized asymmetric Laplace distribution can be used to construct a process with independent and stationary increments – the previously mentioned Laplace motion. The Laplace motion $\Lambda(x)$ is a process that starts at zero and whose distribution at x is given by

$$\phi_{\Lambda(x)}(v) = \mathsf{E}[e^{iv\Lambda(x)}] = \frac{e^{iv\gamma x}}{(1 - i\mu v + \frac{\sigma^2 v^2}{2})^{\frac{x}{\nu}}},$$

where γ is a parameter representing the drift of the process. The Laplace motion can be extended to the whole real line by basically taking two independent copies of it and mirror one of them in the origin. The extended process can then be used to define the moving average (3). Since the increments of the Laplace motion are allowed to have an asymmetric distribution ($\mu \neq 0$) it turns out that also the corresponding moving average process will have a non-symmetric marginal distribution. In fact, the marginal distribution of the Laplace driven MA has the following characteristic function

$$\phi_{Y(t)}(v) = \exp\left(\int_{-\infty}^{\infty} i\gamma v f(x) - \frac{1}{\nu}\log\left(1 - i\mu v f(x) + \frac{\sigma^2 f^2(x) v^2}{2}\right) dx\right), \quad (4)$$

where log is the complex logarithm function.

When it comes to the properties of the Laplace driven MA one can show that the mean and the twosided spectral density $S(\omega)$ are given by

$$\mathsf{E}[Y(t)] = \left(\gamma + \frac{\mu}{\nu}\right)\int_{-\infty}^{\infty} f(x)\,dx, \quad S(\omega) = \frac{\sigma^2 + \mu^2}{\nu}\frac{1}{2\pi}|\mathcal{F}f(\omega)|^2, \quad (5)$$

where $\mathcal{F}$ denotes the Fourier transform. This means that by choosing different kernels one can in principle model any spectrum. However, after having chosen the kernel f and fitted mean and variance there are still two parameters, out of the four original ones, left. These "two degrees of freedom" can e.g. be used to fit skewness s and excess kurtosis κ of the marginal distribution of $Y(t)$. By using the expression for the characteristic function (4) these are given by

$$s = \mu\nu^{1/2}\frac{2\mu^2 + 3\sigma^2}{(\mu^2 + \sigma^2)^{3/2}}\frac{\int_{-\infty}^{\infty} f^3(x)\,dx}{\left(\int_{-\infty}^{\infty} f^2(x)\,dx\right)^{3/2}}, \quad (6)$$

$$\kappa = 3\nu\left(2 - \frac{\sigma^4}{(\mu^2 + \sigma^2)^2}\right)\frac{\int_{-\infty}^{\infty} f^4(x)\,dx}{\left(\int_{-\infty}^{\infty} f^2(x)\,dx\right)^2}. \quad (7)$$

This ability to fit both spectrum and the marginal skewness and kurtosis is hence very promising when it comes to modeling using second order processes. Note that for a Gaussian process both skewness and excess kurtosis equal zero, i.e. $s = \kappa = 0$. In fact, a Gaussian process can be obtained from the Laplace driven MA as a limiting case as $s = 0$ and $\kappa \to 0$, see [20] (page 183). This can be done by first fixing the spectrum (and thus also the kernel) and then letting $\kappa \to 0$.

3.2 Simulation of the Laplace driven MA

The Laplace driven moving average can be simulated in several different ways. The simplest and most straightforward one is to first simulate the increments of the Laplace motion over an equally spaced grid and then convolve it with the kernel f. In full generality, following [20], the asymmetric Laplace motion $\Lambda(x)$ with drift γ can be represented as

$$\Lambda(x) = \gamma \cdot x + \mu\Gamma(x) + B(\Gamma(x)),$$

where $\Gamma(x)$ is a gamma-process characterized by independent and homogeneous dx-increments having a gamma distribution with shape parameter dx/ν and scale parameter 1 while $B(x)$ is Brownian motion with parameter σ. Using this representation a simple algorithm for simulating the Laplace driven moving average with kernel f is given by:

(1) Pick m, and dx so that f is well approximated by its values on $0 < dx < \cdots < m \cdot dx$.
(2) Pick $n \gg 2m - 2$ so the $k = n - 2m + 2$ values of Y will be generated at $0 < dx < 2 \cdot dx < \cdots < k \cdot dx$.
(3) Simulate n i.i.d. $\Gamma(dx/\nu, 1)$ random variables and store them in a vector $G = [G_j]$.
(4) Simulate n i.i.d. zero mean standard normal random variables and store them in a vector Z.
(5) Compute $Y = \gamma \int f(x)\,dx + \mu f * G + \sigma f * (\sqrt{G} \cdot Z)$, where $\sqrt{G} \cdot Z = [\sqrt{G_j} \cdot Z_j]$, $*$ denotes convolution (we extend to infinite sequences by setting zero to the entries that have not been set otherwise), and the integral $\int f(x)\,dx$ is computed by some numerical method.
(6) Remove the first $m - 1$ and last $m - 1$ entries of the vector Y. The resulting vector Y is a simulation of the Laplace driven moving average with parameters μ, ν, σ and drift γ.

The advantage with this simulation method is that it is very fast and efficient and that it works for long simulations and for most values of the parameters. The disadvantage is that one looses some resolution on where the jumps in the Gamma process occurs, due to taking an equally spaced grid. In Figure 2

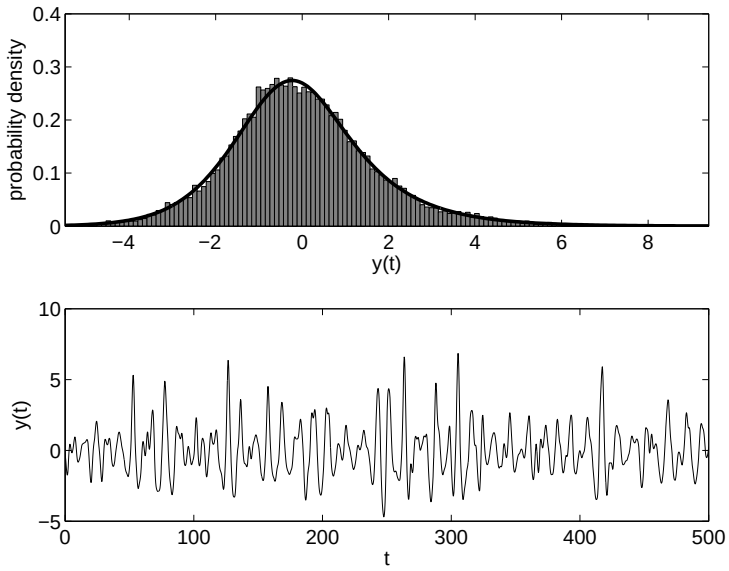

Fig. 2. Simulation of a zero mean Laplace driven MA having a Pierson-Moskowitz spectrum with significant waveheight 7 m and peak period 11 s. A symmetric kernel f satisfying $\int f^2(x)\,dx = 1$ is used and the values of skewness and excess kurtosis are $s = 0.6$ and $\kappa = 2$. This corresponds to parameters $\nu = 1.96$, $\sigma = 1.45$, $\mu = 1.98$ and $\gamma = -\mu/\nu = -1.01$. In the top panel a histogram and the theoretical density, computed by numerical Fourier inversion of the characteristic function, are shown. A piece of the simulation of Y is shown in the lower panel.

a simulation of the Laplace MA is shown for a Pierson-Moskowitz spectrum, see [21].

3.3 Rice's formula

In order to compute the upper bound (A.3) for the damage the upcrossing intensity has to be computed. According to Rice's formula (2) this can be done as long as the joint density of $Y(0)$ and $\dot{Y}(0)$ is available. In the case of the Laplace driven MA one cannot find an explicit formula for this density. However, one can find one for the joint characteristic function, viz.

$$\begin{aligned}\phi_{Y(0),\dot{Y}(0)}(v_1,v_2) &= \exp\left(i\gamma\int_{-\infty}^{\infty} v_1 f(x) + v_2\dot{f}(x)\,dx\right)\\ \cdot\exp&\left(-\frac{1}{\nu}\int_{-\infty}^{\infty}\log\left(1 - i\mu(v_1 f(x) + v_2\dot{f}(x)) + \frac{\sigma^2}{2}(v_1 f(x) + v_2\dot{f}(x))^2\right)\,dx\right),\end{aligned} \tag{8}$$

where log denotes the complex logarithm function. That this expression holds is easiest seen by noting that

$$v_1 Y(0) + v_2 \dot{Y}(0) = \int_{-\infty}^{\infty} (v_1 f(x) + v_2 \dot{f}(x))\, d\Lambda(x)$$

and using (4). Using the characteristic function (8), we express the upcrossing intensity by

$$\mu^+(u) = \frac{1}{(2\pi)^2} \int_0^{\infty} \int_{-\infty}^{\infty} \int_{-\infty}^{\infty} z\, e^{-i(v_1 u + v_2 z)} \phi_{Y(0),\dot{Y}(0)}(t_1, t_2)\, dv_1\, dv_2\, dz. \qquad (9)$$

The upcrossing intensity is not given by an explicit formula and thus must be evaluated numerically. In this paper we apply the two-dimensional fast Fourier transform algorithm combined with the trapezoidal method.

3.4 Laplace driven MA and linear filters

Another convenience of the Laplace driven MA is its natural behavior when passed through a linear filter. Let $h(x)$ be the impulse response of a linear filter. Then, by changing the order of integration,

$$\begin{aligned} h * Y(t) &= \int_{-\infty}^{\infty} h(t-s) Y(s)\, ds = \int_{-\infty}^{\infty} \int_{-\infty}^{\infty} h(t-s) f(s-x) d\Lambda(x)\, ds \\ &= \int_{-\infty}^{\infty} \left(\int_{-\infty}^{\infty} h(t-s) f(s-x)\, ds \right) d\Lambda(x) = \int_{-\infty}^{\infty} h * f(t-x)\, d\Lambda(x). \end{aligned}$$

Hence, by filtering a Laplace MA with kernel f one gets back a Laplace MA but now with kernel $h * f$, see Figure 3. This means e.g. that if one can compute crossing intensity for the Laplace MA, and thereby the upper bound (A.3) for the damage, see the appendix, one can also do it in the same manner for linearly filtered Laplace MA.

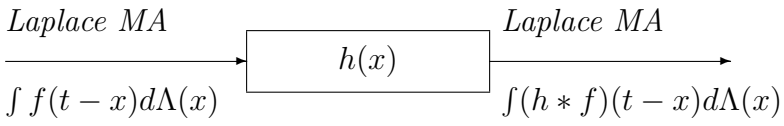

Fig. 3. Input-output relation.

Note that as the process is filtered the spectrum is multiplied by $|H(\omega)|^2$ as for Gaussian loads but the parameters ν, σ, μ and γ for the Laplace motion $\Lambda(x)$ remain unchanged. However, skewness and kurtosis of the filtered process change since by virtue of (6) and (7) these quantities are a function of the kernel which in the filtered process is $h * f$.

4 Examples

In this section we illustrate the proposed model by estimating the expected damage both for stiff structures and structures having dynamics well described by a linear oscillator. The load acting on the structure is modeled by a Laplace driven moving average process.

4.1 Simulation experiment

In order to illustrate the new model and also to evaluate the performance of the upper bound for the damage, given in (A.3) of the appendix, the following simulation experiment is done. In the first take, the structure on which the load is acting is supposed to be stiff, i.e. stresses are proportional to the applied load. Here, for simplicity, the coefficient of proportionality is set to one. The load $Y(t)$ is modeled by a Laplace driven moving average having parameters ν, σ, μ and γ and a symmetric kernel f corresponding to a spectrum of the Pierson-Moskowitz type. The same spectrum is used throughout the experiment and the significant wave height is set to 7 m and the peak period to 11 s, see Figure 4.

The damage intensity on the structure, that is the accumulated damage per time unit, can be estimated in two different ways: either by direct simulation of the response and computing the observed rainflow damage according to (1); or by direct computation of the upper bound (A.3) for the damage without making any simulations. In Table 1 the simulated damage intensity and the upper bound (A.3) for the Laplace driven MA are shown for different values of skewness and kurtosis. The simulated values are computed as a mean over 1000 independent simulations, each consisting of $10,000$ data points sampled at 1.85 Hz. For comparison the simulated damage and the upper bound in the Gaussian model (A.5) are also computed. The Gaussian model clearly causes much less damage compared to the Laplace driven MA for large values of s and κ in combination with high values of the fatigue exponent β, mainly due to the fact that the Gaussian distribution has too light tails and thus does not include enough big cycles. Moreover, the upper bound seems to follow the simulated values closesly, both for the Laplace and the Gaussian model, see also Figure 5. This has to do with to the fact that the spectrum is fairly narrow-banded, at least from a fatigue application point of view. As skewness and excess kurtosis are close to zero the simulations from the two models are close, as can be expected since the Laplace model converges to a Gaussian process as $\kappa \to 0$. However, the Laplace upper bound is not in perfect agreement with the Gaussian upper bound because of numerical problems when computing the crossing intensity (9). These problems arise since one has to choose a finite

	Laplace model						Gaussian model	
β	$s=0$, $\kappa=0.01$		$s=0.3$, $\kappa=1$		$s=0.6$, $\kappa=2$		$s=0$, $\kappa=0$	
2	2.89	**3.16**	2.93	**3.16**	2.90	**3.08**	2.90	**3.06**
3	18.6	**19.6**	21.0	**21.8**	22.1	**22.4**	18.7	**20.1**
4	135	**146**	180	**190**	207	**211**	135	**149**
5	1080	**1200**	1790	**1940**	2300	**2350**	1080	**1230**
6	9430	**10700**	20100	**22500**	29600	**30400**	9380	**11000**

Table 1
Estimated fatigue damage intensity for a stiff structure subjected to a Laplace driven MA load for different values of skewness s, excess kurtosis κ and fatigue exponent β. Simulations are given in plain text and the upper bounds in bold text. The last two columns give the corresponding values for a Gaussian load.

grid to evaluate the characteristic function on before computing the crossing intensity. If the grid is not fine enough the crossing intensity is underestimated and thereby also the upper bound.

Next the experiment is repeated. However, this time the load is supposed to be acting on a structure having dynamics described by a linear damped oscillator, i.e. having dynamics that is described by the following differential equation

$$Z''(t) + 2zw_0Z'(t) + w_0^2Z(t) = \frac{1}{m}Y(t),$$

where $Z(t)$ is the response and $Y(t)$ the load. The parameters have the following interpretation: w_0 is the resonance frequency of the undamped system, z is a damping coefficient and m equals the mass that is accelerated. The transfer function $H(\omega)$ is in this case given by

$$H(\omega) = \frac{1/m}{-\omega^2 + 2z\omega_0 i\omega + \omega_0^2}.$$

If the load $Y(t)$ is a Laplace driven MA then, due to the properties of this class of models, the response $Z(t)$ is also a Laplace driven MA. However, the kernel of $Z(t)$ is $h * f(t)$, where f is the kernel of $Y(t)$ and $h = \mathcal{F}^{-1}H$ is the causal impulse response of the linear oscillator. Moreover the parameters σ, ν, μ and γ remain unchanged whereas the values of skewness and kurtosis change according to (6) and (7).

The same spectrum is used for the load as in the previous example, namely a Pierson-Moskowitz spectrum with significant wave heigth 7 m and peak period 11 s and the parameters of the oscillator are, for illustration reasons, set to $m = 0.37$ kg, $\omega_0 = 2$ rad/s and $z = 0.05$. The resulting spectrum of the output

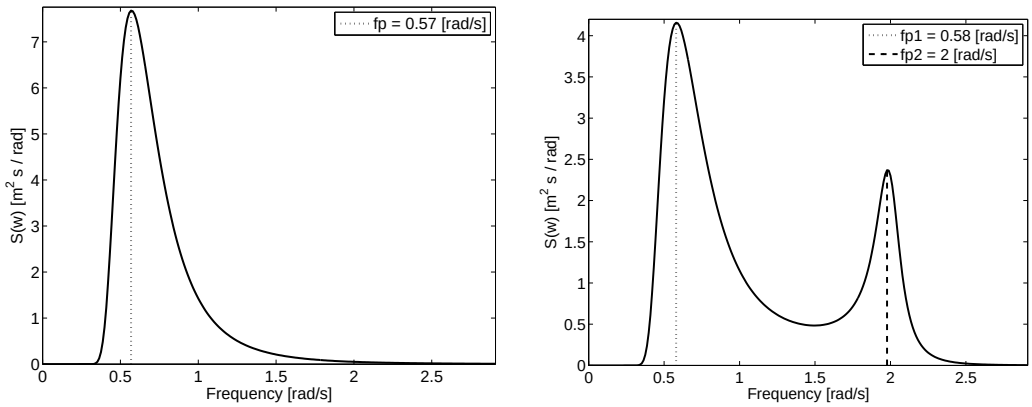

Fig. 4. Spectrum of the input process in the left panel and the filtered process in the right one.

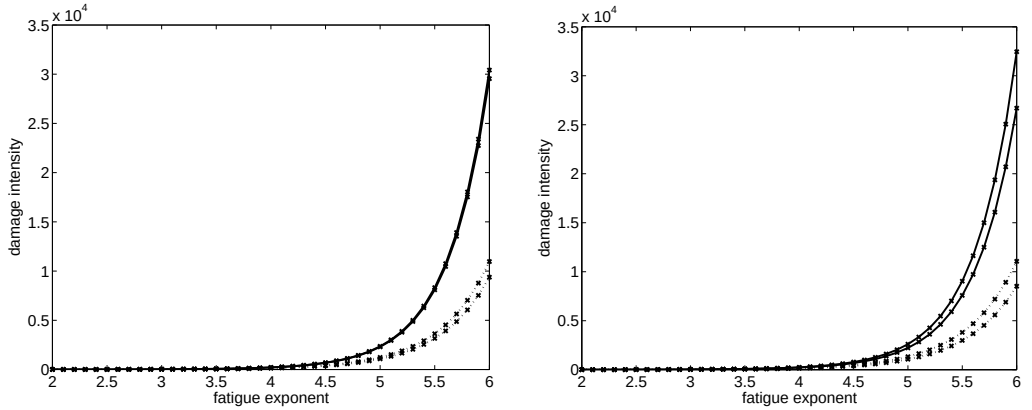

Fig. 5. Damage intensity for a stiff structure (left) and a linear oscillator (right) driven by Laplace MA with skewness $s = 0.6$ and excess kurtosis $\kappa = 2$. Simulated damage intensity (solid), upper bound according to Laplace MA model (dashed) and upper bound from Gaussian model (dotted).

process $Z(t)$ is shown in Figure 4. The first peak can be thought of as the stress induced by e.g. ocean waves and the second peak as the stress induced by resonances in the structure. In Table 2 the damage intensity is shown for the filtered process. Again the values corresponds to direct simulation and the upper bound (A.3) for the Laplace driven MA and the corresponding quantities for a Gaussian process having the same spectral density function. The values of s and κ refer in this case to the skewness and excess kurtosis of the process driving the oscillator. The biggest difference in this case, compared to the stiff structure in Table 1, is that the upper bound differs more from the simulated values. This is due to the broadband character of the spectrum. Keeping in mind that the upper bound (A.3) has the interpretation of being a narrow-band approximation, at least in the Gaussian case, this is not so surprising. In Figure 5 the simulated damage is compared to the Laplace MA upper bounds for excess kurtosis $\kappa = 2$ and skewness $s = 0.6$.

	Laplace model						Gaussian model	
β	$s=0$, $\kappa=0.01$		$s=0.3$, $\kappa=1$		$s=0.6$, $\kappa=2$		$s=0$, $\kappa=0$	
2	3.62	**4.12**	3.61	**4.10**	3.59	**4.06**	3.63	**4.13**
3	21.3	**24.3**	23.3	**26.4**	24.7	**27.9**	21.4	**25.2**
4	143	**167**	182	**197**	215	**246**	144	**174**
5	1060	**1270**	1660	**1970**	2220	**2610**	1060	**1330**
6	8540	**10500**	17100	**21100**	26700	**32500**	8520	**11100**

Table 2
Estimated fatigue damage intensity for a linear oscillator subjected to a Laplace driven MA load for different values of skewness s, excess kurtosis κ and fatigue exponent β. Simulations are given in plain text and the upper bounds in bold text. The last two columns give the corresponding values for a Gaussian load.

4.2 The effect of skewness and kurtosis on fatigue damage

This example illustrates the effect of skewness and kurtosis on the accumulated damage. Moreover it shows the danger of using a Gaussian model when not appropriate. Again the Pierson-Moskowitz spectrum in Figure 4 is used and the accumulated damage for the Laplace driven MA is computed by simulations for different values of skewness and kurtosis. These values are then compared to what is obtained in a Gaussian model by forming the ratio

$$\lambda = \frac{\mathsf{E}[D_{LMA}]}{\mathsf{E}[D_G]},$$

where D_{LMA} and D_G are the accumulated damages in the Laplace and Gaussian models respectively. In Figure 6 λ is shown as a function of skewness and excess kurtosis. Each value is computed as a mean of 1000 simulations each of length $10,000$ having sample frequency 3.7 Hz. On one hand, for fixed skewness, the damage increases with excess kurtosis. On the other hand, for fixed kurtosis, the damage is decreasing with the absolute value of the skewness, a fact that also was reported by [6] for another type of model. Moreover the damage is clearly symmetric in the skewness parameter. This is a result of the particular damage function used here which is symmetric in the rainflow minima and maxima. As noted in [4] one can by including the mean stress in the damage function get a damage that is an asymmetric function of skewness with the highest damage for some positive value of the skewness parameter.

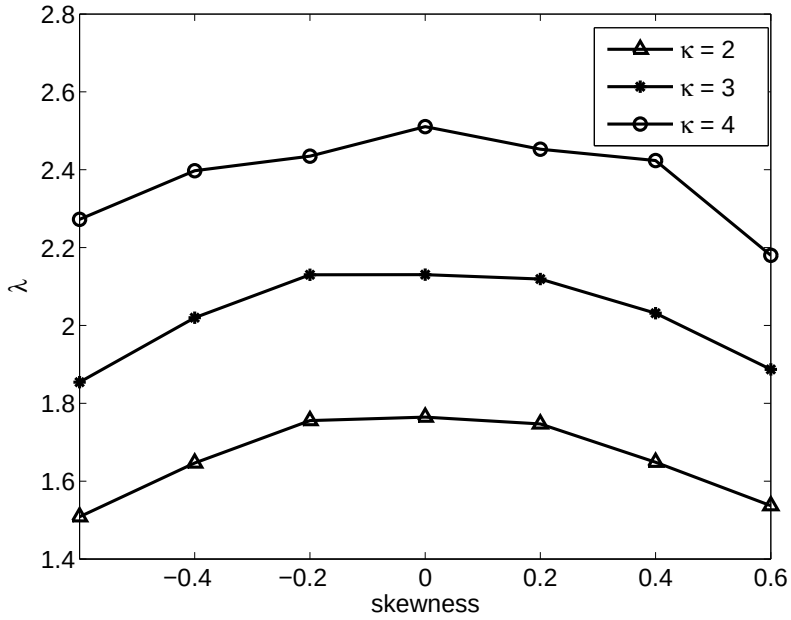

Fig. 6. Laplace to Gaussian fatigue damage ratio λ as a function of skewness and excess kurtosis.

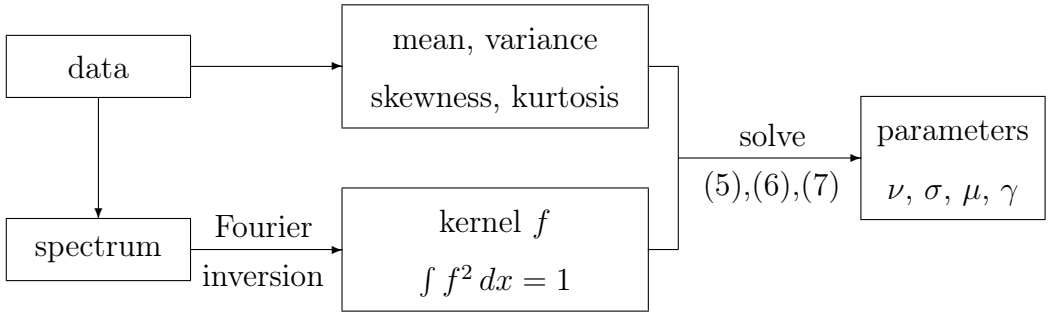

Fig. 7. Estimation procedure. First the spectrum is estimated from data and a kernel is found by Fourier inversion. Then mean, variance, skewness and kurtosis are estimated and equations (5), (6) and (7) are used, together with the kernel, to solve for the Laplace parameters ν, σ, μ and γ.

4.3 Example with real data

This example deals with a data set consisiting of sea surface elevation measurements, measured at a platform off the west African coast. The platform is located at shallow water so the data might be expected to deviate from the Gaussian model. The data set contains 9524 data points sampled at 4 Hz.

The Laplace MA model is fitted to the data. In order to do so the spectral density is first estimated from data and after that a symmetric kernel satisfying $\int f^2\,dx = 1$ is determined according to (5) by using Fourier inversion, see

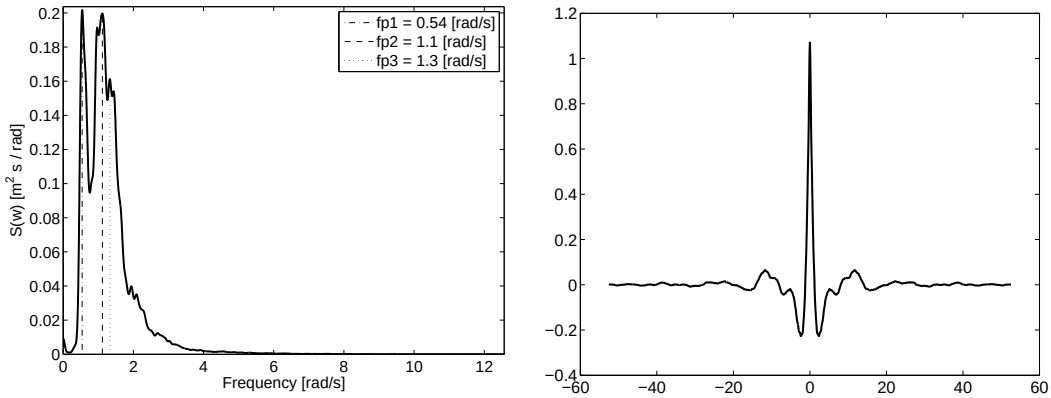

Fig. 8. Estimated spectral density function for the "africa" data (left) and estimated kernel function (right).

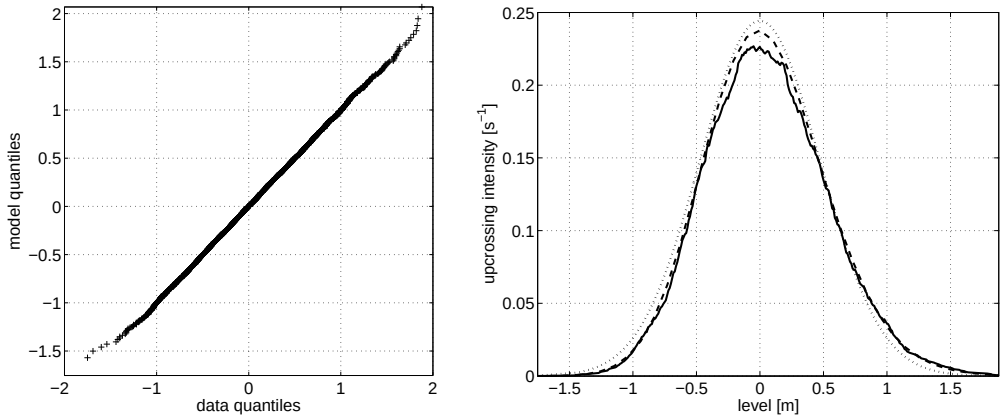

Fig. 9. Quantile-quantile plot of africa data and fitted model (left) and upcrossing intensity (right) of data (solid line), Laplace model (dashed line) and corresponding Gaussian model (dotted line).

Figure 8. The rest of the parameters are fitted using a moment matching approach, i.e. by estimating mean, variance, skewness and kurtosis and solving (5), (6) and (7) for the paramters ν, σ, μ and γ. The skewness and excess kurtosis were in this case estimated to $s = 0.25$ and $\kappa = 0.17$. Thus this data set is skewed and has somewhat heavier tails than the Gaussian distribution. A scheme of the estimation procedure is shown if Figure 7. The fit of the model to the data is good both when it comes to marginal distribution and crossing intensity, see Figure 9.

Now assume that this load is acting on a stiff structure in the same fashion as in the previous simulation experiment. In Figure 10 the observered damage intensity and the damage intensity simulated by the Laplace and Gaussian models are shown. The simulated values are computed as the sample mean of 100 simulations each consisting of 9524 data points sampled at frequency 4 Hz. Clearly the values simulated from the Laplace driven MA model give a very good estimate of the expected damage intensity, whereas the Gaussian

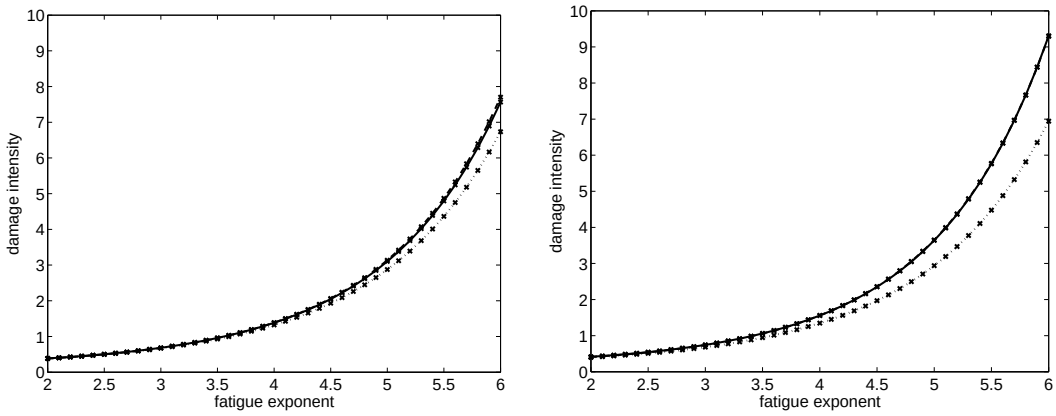

Fig. 10. Fatigue damage intensity for a stiff structure subjucted to ocean waves. The damage is comupted using a symmetric damage function (left) and a mean stress corrected damage function (right). Observed damage (dashed), simulated damage in Laplace driven MA model (solid), and simulated damage in Gaussian model (dotted).

model has a tendency to underestimate the damage. The difference between the models is however quite small, a fact that may be explained by the values of skewness and excess kurtosis which in this case are $s = 0.25$ and $\kappa = 0.17$. Based on the experience from the previous simulation experiment it is known that the Gaussian and the Laplace MA models give similar values for the damage when both skewness and excess kurtosis are close to zero. As the kurtosis increases the damage will also increase. However, as a result of the curve in Figure 6, this effect can to some extent be reduced by also increasing the skewness. Therefore a Laplace model with small kurtosis and relatively large skewness, as is the case here, will give rise to similar damage as a Gaussian model.

So, does this mean that the two models in this case are almost equivalent? The answer to that question depends on what damage function one uses in the rainflow analysis. In Figure 11 rainflow minima are plotted against rainflow maxima for the observed data and simulations from the Laplace and Gaussian models. Apparently the Laplace model better models the rainflow cycles. However, it turns out that this difference does not show up in the cycle range distribution but rather in the cycle mean distribution. Thus, if a damage function that only uses the cycle range is used the Laplace and the Gaussian models will in this case be nearly equivalent whereas a mean stress corrected damage function will lead to a bigger difference. A simple way to include the mean stress in the damage function, sometimes referred to as mean stress sensibility, is to use a corrected cycle range S_c, say, defined by

$$S_c = (v_i - u_i^{rfc}) + M(v_i + u_i^{rfc}),$$

where (u_i^{rfc}, v_i) are the rainflow cycles and M is a material parameter. The damage function is then defined by $f(u_i^{rfc}, v_i) = S_c^{\beta}$. Using this particular damage function with $M = 0.3$, see Figure 10, the difference between the

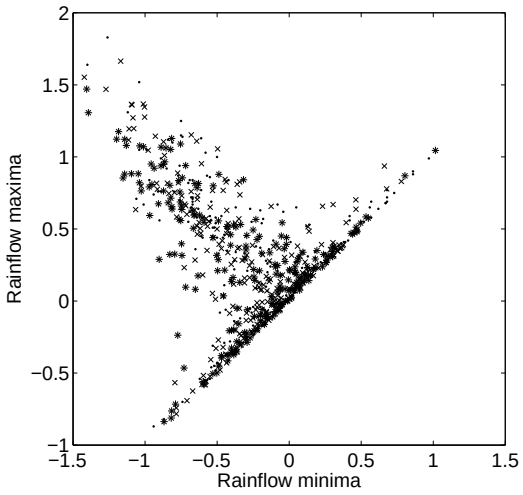

Fig. 11. Rainflow minima plotted against rainflow maxima. Observed data (dots), simulation from Laplace model (crosses) and from Gaussian model (stars).

models increases as expected.

5 Conclusions

A new model for random loads, the Laplace driven moving average, has been presented. The model is a non-Gaussian stationary process possessing a spectral density function. Moreover it also has additional degrees of freedom so that one e.g. can model the skewness and kurtosis of the marginal distribution. Thus, for the proposed class of random loads, one can easily vary spectrum, skewness and kurtosis parameters and consequently fit a variety of possible loading conditions.

Another property of the proposed class of models is that it is closed under linear filtration. This means that if a Laplace driven MA is used as input to a linear filter the output process will also be a Laplace driven MA. This is an important advantage in comparison to other non-Gaussian models such as e.g. transformed Gaussian processes.

The fatigue damage due to a Laplace driven MA can be either computed by direct simulation or bounded from above using an expression relying on the upcrossing intensity. In our simulation example it has been shown that the upper bound is a good option when the spectrum is narrow-banded whereas it can be too crude in other situations. Moreover the new model has been used to show the effect of skewness and kurtosis on fatigue damage, and the results are similar to what has been seen in other studies namely that the fatigue damage increases with kurtosis and decreases with the absolute value of the skewness. Usefulness for modelling real data has been demonstrated using sea

surface elevation data. For the particular data set used, the model gave a good description of the rainflow maxima and minima and thereby also an accurate analysis of the fatigue damage.

6 Acknowledgement

Research supported in part by the Gothenburg Stochastic Center and the Swedish foundation for Strategic Research through GMMC, Gothenburg Mathematical Modelling Center.

A Fatigue damage and level crossings

As previously mentioned the fatigue damage may be computed according to

$$D(T) = \sum f(u_i^{\text{rfc}}, v_i) + D^{\text{res}},$$

where $f(u_i^{\text{rfc}}, v_i)$ is the fatigue damage due to the ith rainflow pair and D^{res} is the damage caused by cycles found in the residual. An alternative way of computing rainflow damage is by means of counting interval upcrossings $N_T^+(u, v)$, say. The number of upcrossings $N_T^+(u, v)$ of an interval $[u, v]$ by a continuous function $y(t)$, $0 \leq t \leq T$, is defined as the largest index n such that there are times $0 \leq s_1 < t_1 < s_2 < \ldots < s_n < t_n$ satisfying $y(s_i) < u \leq v < y(t_i)$ and $s_n \leq T$, see Figure A.1 for an illustration. Upcrossings of the interval $[u, u]$ are just upcrossings of the level u and are denoted by $N_T^+(u)$.

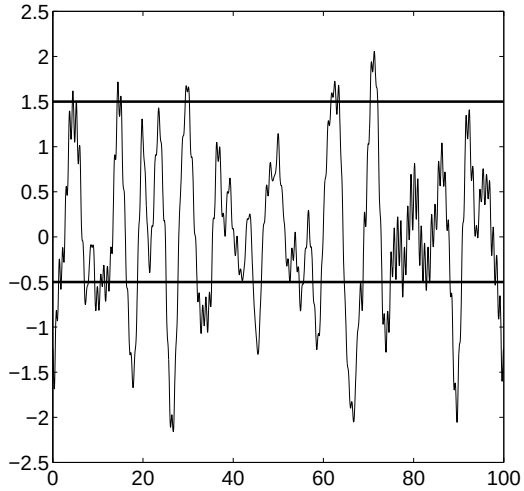

Fig. A.1. Upcrossings of the interval $[-0.5, 1.5]$. In this case $N_{100}^+(u, v) = 5$.

As was proven in [22], the rainflow damage can be written in terms of interval upcrossings. Let $f(u, v) = \alpha\,(v - u)^\beta$ be the damage caused by a single cycle.

Then

$$D(T) = -\int_{-\infty}^{+\infty}\int_{-\infty}^{y} \frac{\partial^2 f(x,y)}{\partial x \partial y} N_T^+(x,y)\,dx\,dy - \int_{-\infty}^{+\infty} \left.\frac{\partial f(x,y)}{\partial x}\right|_{y=x} N_T^+(x)\,dx$$

is the total damage. If the load Y is random one is rather interested in the expected damage given by

$$E[D(T)] = -\int_{-\infty}^{+\infty}\int_{-\infty}^{y} \frac{\partial^2 f(x,y)}{\partial x \partial y} E[N_T^+(x,y)]\,dx\,dy - \int_{-\infty}^{+\infty} \left.\frac{\partial f(x,y)}{\partial x}\right|_{y=x} E[N_T^+(x)]\,dx. \quad \text{(A.1)}$$

For a stationary load Y the expected number of interval crossings becomes

$$E[N_T^+(u,v)] = T\,E[N_1^+(u,v)] = T\,\mu^+(u,v),$$

where $\mu^+(u,v)$ is the intensity of interval upcrossings. Similarly, $E[N_T^+(u)] = T\,E[N_1^+(u)] = T\,\mu^+(u)$. Thus, considering equation (A.1), the key to compute the expected damage is to know the intensity of upcrossings of intervals for the random load at hand. Unfortunately, it is in most cases very hard to compute this intensity and explicit formulas are known only for loads satisfying a Markov condition. One possibility to avoid this problem is to bound $\mu^+(u,v)$ from above in the following manner

$$\mu^+(u,v) \le \min_{u\le z\le v} \mu^+(z) = k(u,v). \quad \text{(A.2)}$$

This simplifies the problem since as long as the joint density of $Y(0), \dot{Y}(0)$ is known the upcrossing intensity $\mu^+(u)$, and thereby also $k(u,v)$, can be computed by means of the celebrated Rice's formula [19]. Using the upper bound (A.2) for $f(u,v) = \alpha\,(v-u)^\beta$ with $\beta > 1$, the expected rainflow damage can be bounded by

$$E[D(T)] \le T\alpha\beta(\beta-1)\int_{-\infty}^{+\infty}\int_{-\infty}^{y} (y-x)^{\beta-2} k(x,y)\,dx\,dy. \quad \text{(A.3)}$$

For a stationary Gaussian load the upper bound (A.3) takes a particularly simple form, see [23], and equals a narrow band approximation proposed by Bendat, [24], at a time when a definition for the rainflow cycle counting was not yet available. For a zero mean stationary random load Bendat proposed that the cycle amplitude H, say, has the following probability distribution

$$P(H \le z) = 1 - \frac{\mu^+(z)}{\mu^+(0)}. \quad \text{(A.4)}$$

Moreover, he proposed to approximate the intensity of cycles by means of $f_z = \mu^+(0)$, called the apparent frequency. This method is applicable not

only for Gaussian loads but for all loads having a unimodal and symmetric upcrossing intensity $\mu^+(z)$. The distribution (A.4) of the cycle amplitude was then used to compute the average damage which is called the narrow band approximation

$$E[D^{nb}(T)] = T\,\alpha\,f_z\,E(2H)^\beta.$$

For a zero mean Gaussian load having spectrum $S(\omega)$ and spectral moments defined by $\lambda_i = \int_{-\infty}^{+\infty} \omega^i\,S(\omega)\,d\omega$ it follows from Rice's formula that H has a Rayleigh distribution, i.e. $H = \sqrt{\lambda_0}R$ where $P(R \le r) = 1 - e^{-r^2/2}$. Furthermore $f_z = (2\pi)^{-1}\sqrt{\lambda_2/\lambda_0}$. Using these facts the narrow band approximation of the expected damage for Gaussian loads, often used in offshore applications, becomes

$$E[D(T)] \approx E[D^{nb}(T)] = T\,\alpha f_z E[(2\sqrt{\lambda_0}R)^\beta] = T\alpha\,f_z\,h_s^\beta\,2^{-\beta/2}\Gamma(1+\beta/2), \tag{A.5}$$

where $h_s = 4\sqrt{\lambda_0}$ is the so called significant amplitude while $\Gamma(x)$ is the gamma function defined by $\Gamma(x) = \int_0^{+\infty} s^{(x-1)}\exp(-s)\,ds$.

References

[1] Z. Gao, T. Moan, Fatigue damage induced by nonGaussian bimodal wave loading in mooring lines, Appl. Ocean Res. 29 (2007) 45–54.

[2] S. Sarkani, D. P. Kihl, J. E. Beach, Fatigue of welded joints under narrowband non-gaussian loadings., Probabilist. Eng. Mech. 9 (1994) 179–190.

[3] D. P. Kihl, S. Sarkani, J. E. Beach, Stochastic fatigue damage accumulation under broadband loadings, Int. J. Fatigue 17 (1995) 321–329.

[4] S. Wang, J. Q. Sun, Effect of skewness on fatigue life with mean stress correction, J. Sound Vib. 282 (2005) 1231–1237.

[5] D. Benasciutti, R. Tovo, Fatigue life assessment in non-Gaussian random loadings, Int. J. Fatigue 28 (2006) 733–746.

[6] L. Yu, P. K. Das, N. P. D. Barltrop, A new look at the effect of bandwidth and non-normality on fatigue damage, Fatigue Fract. Eng. M. 27 (2004) 51–58.

[7] S. R. Winterstein, Non-normal responses and fatigue damage, J. Eng. Mech.-ASCE 111 (1985) 1291–1295.

[8] S. R. Winterstein, O. B. Ness, Hermite moment analysis of nonlinear random vibration, in: W. K. Liu, T. Belytschko (Eds.), Computational Mechanics of Probabilistic and Reliability Analysis, Elme Press, 1989, Ch. 21, pp. 452–478.

[9] M. K. Ochi, K. Ahn, Probability distribution applicable to non-Gaussian random processes., Probabilist. Eng. Mech. 9 (1994) 255–264.

[10] U. E. B. Machado, Probability density functions for nonlinear random waves and responses, Ocean Eng. 30 (2003) 1027–1050.

[11] I. Rychlik, P. Johannesson, M. R. Leadbetter, Modelling and statistical analysis of ocean-wave data using transformed Gaussian processes, Mar. Struct. 10 (1997) 13–47.

[12] K. Bogsjö, Road profile statistics relevant for vehicle fatigue, Ph.D. thesis, Lund University (2007).

[13] K. R. Gurley, A. Kareem, M. A. Tognarelli, Simulation of a class of non-normal random processes, Int. J. Nonlinear Mech. 31 (1996) 601–617.

[14] A. Naess, O. Gaidai, The asymptotic behaviour of second-order stochastic Volterra series models of slow drift response, Probabilist. Eng. Mech. 22 (2007) 343–352.

[15] M. Matsuishi, T. Endo, Fatigue of metals subjected to varying stresses, Paper presented to Japan Soc. Mech. Engrs, Jukvoka, Japan (March 1968).

[16] I. Rychlik, A new definition of the rainflow cycle counting method, Int. J. Fatigue 9 (1987) 119–121.

[17] A. Palmgren, Die Lebensdauer von Kugellagern, VDI Zeitschrift 68 339–341.

[18] M. A. Miner, Cumulative damage in fatigue, J. Appl. Mech. 12 (1945) A159–A164.

[19] S. O. Rice, The mathematical analysis of random noise i and ii, Bell Syst. Tech. J. 23, 24 (1944, 1945) 282–332, 46–156.

[20] S. Kotz, T. J. Kozubowski, K. Podgórski, The Laplace distribution and generalizations: A revisit with applications to communications, economics, engineering and finance, Birkhäuser, Boston, 2001.

[21] W. J. Pierson, L. Moskowitz, A proposed spectral form for fully developed wind seas based on the similarity theory of S.A. Kitaigordskii, J. Geophys. Res. 69 (1964) 5181–5190.

[22] I. Rychlik, Note on cycle counts in irregular loads, Fatigue Fract. Eng. M. 16 (1993) 377–390.

[23] I. Rychlik, On the "narrow-band" approximation for expected fatigue damage, Probabilist. Eng. Mech. 8 (1993) 1–4.

[24] J. S. Bendat, Probability functions for random responses: Prediction of peaks, fatigue damage and catastrophic failures, Tech. rep., NASA (1964).